



Optical, structural and electrical properties of ZnO thin films doped with Mn

Alejandra López-Suárez¹ · Dwight Acosta¹ · Carlos Magaña¹ · Francisco Hernández¹

Received: 9 October 2019 / Accepted: 26 December 2019 / Published online: 8 January 2020
© Springer Science+Business Media, LLC, part of Springer Nature 2020

Abstract

Manganese-doped zinc oxide (Mn-doped ZnO) thin films were synthesized on soda lime glass substrates using the spray pyrolysis technique at substrate temperatures of 400, 450 and 500 °C. Compositional, optical, structural, morphological and electrical properties were studied with Rutherford Backscattering Spectrometry (RBS), Ultraviolet and Visible Spectroscopy (UVS), X-Ray Diffraction (XRD) analysis, Scanning Electron Microscopy (SEM) and the Four Point method, respectively. Mn-doped ZnO films show changes in transmittance and energy band gap when substrate temperature is increased. In the same way, electrical resistivity measurements show changes with temperature, getting a minimum value at 450 °C. The results were also compared with undoped ZnO thin films. They show that constant lattices, crystallite size and resistivity increase with Mn doping. These variations are the result of the substitution of Zn by Mn ions during the incorporation of Mn ions in the ZnO lattice. On the other hand, energy band gap values decrease when the samples were doped with Mn, due to the *s*–*d* and *p*–*d* exchange interactions.

1 Introduction

Zinc oxide (ZnO) is considered one of the most important semiconductors used for many applications in microelectronics, optoelectronic devices, heat mirrors, transparent electrodes, blue/UV light-emitter devices, etc. This is because to its large band gap around 3.37 eV, its large excitation binding energy of 60 meV and on its properties such as high catalytic activity, chemical stability, piezoelectricity and high-optical transparency in the visible region.

Photovoltaic energy is a promising source of energy that could be used as a possible substitute for electrical energy produced by conventional methods. For this reason, there is a great interest to obtain semiconductor films, transparent and cheap to be used in solar cells systems. ZnO is a transparent semiconductor, which has great advantages over other materials due to its high thermal stability, its low price and its non-toxicity [1].

Different properties of ZnO-like optical absorbance, band gap energy, resistivity, melting point or ferromagnetism can be tailored by adding dopant ions into the film, making the

material an ideal candidate for applications such as liquid crystal monitors, piezoelectric sensors and blue light-emitting diodes, among others [2, 3].

Some research groups has been working on doping ZnO thin films with different elements, such as Mn, Al, Co, In to modify the properties of the material [4–8]. In all the cases, improvements in optical, electrical, magnetic and structural properties have been reported. Doping ZnO with Mn facilitates its incorporation into its lattice because there is a minimum difference between the ionic radii of Mn and Zn.

The main purpose of doping ZnO with Mn is to explore the possibility of tailoring the electrical, optical and magnetic properties of ZnO thin films, and to evaluate or analyze new applications in the areas of electronics, optoelectronics, optical devices, among others. Mn-doped ZnO has the potential to become a material in which the magnetic, semi-conducting and optical properties might coexist. Another application of Mn-doped ZnO is tuning the band gap to produce UV detectors and light emitters [9].

ZnO thin films can be synthesized by physical (vapor deposition, laser ablation, and sputtering) and chemical techniques (spray pyrolysis, chemical vapor deposition, sol–gel) [10, 11]. The spray pyrolysis method is a very simple and low-cost process used to synthesize thin films of any composition. The main equipment is composed by an atomizer, precursor solutions, a substrate heater and a

✉ Alejandra López-Suárez
chipi72@gmail.com

¹ Instituto de Física, Universidad Nacional Autónoma de México, 04510 Ciudad de México, Mexico

temperature controller. Within this process, the most relevant is the generation of the aerosol and its transport to the hot substrate, where the film growth occurs. A detailed exposition of the process and the equipment used in the spray pyrolysis technique, can be consulted in Ref. [12].

In the present study, Mn-doped ZnO thin films were synthesized by the spray pyrolysis technique, using substrate temperature of 400, 450 and 500 °C. The evaluation of the effect of the Mn doping together with substrate temperature on the ZnO microstructure, band gap, grain growth and electrical properties is presented.

2 Experimental

Mn-doped ZnO (ZnO:Mn) thin films were deposited by spray pyrolysis technique onto soda lime glass substrates. The spraying solution was prepared by dissolving 10.97 g of zinc acetate 2-hydrated in 250 ml of deionized water. Until dissolution was completed, 50 ml of acetic acid was added slowly under agitation and afterwards 700 ml of ethanol was incorporated to the solution. Manganese chloride (0.05 M) was used to synthesize the Mn-doped ZnO films. Depositions were performed for three substrate temperatures: 400, 450 and 500 °C. The nozzle to substrate distance was 30 cm. During the spraying process cycles of 3 s followed by short periods of 5 s without spraying, to avoid the substrate cooling, were carried out.

To obtain the atomic elemental concentrations of the samples and the films' thickness, RBS analysis was performed. The experiment was conducted in the 3MV Pelletron accelerator of the Instituto de Física, UNAM. Alpha particles coming from a beam of 3 MeV and 1 mm of diameter collide with the elements that compose the sample and scatter at an angle of 167°. After collision, backscattered alpha particles were measured with a surface barrier detector. The RBS spectrum is formed by the analog signals that leave the detector and is processed by a multichannel analyzer. The SIMNRA code [13] was used to simulate and analyze the RBS spectra.

XRD analysis was used to study the structural properties of the ZnO:Mn films. The analysis was carried out in a Bruker D8 Advanced Diffractometer, using the Cu k_{α} radiation. Absorbance and transmittance studies of the samples were performed at room temperature with an Agilent HP 8453 UV–Vis spectrophotometer in the 300–1000 nm range. The morphology of the samples as well as the particle size of the materials were conducted using a Scanning Electron Microscope FEG JEOL JSM-7800. Resistivity measurements were carried out with a Jandel Multi Height Microposition probe equipment, using the four-points probe method.

3 Results and discussion

3.1 RBS results

In a Rutherford Backscattering experiment, alpha particles used as projectiles, collide with the elements that form the sample. When a collision between a projectile and a nucleus takes place, the projectile transfers part of its energy to the atom of the sample, losing energy. In the same way, when the projectile moves across the material, it interacts with the electrons of the atoms that compose the material and loses part of its energy. The energy loss is related to the stopping power of the projectile. If the stopping power of the alpha particles is obtained and the energy loss of the projectiles is measured directly from the RBS spectrum, then the thickness of the film (X) can be calculated with Eq. 1 [14].

$$X = \frac{\Delta E}{[\epsilon]} \quad (1)$$

where ΔE is the energy loss of the alpha particles in the elements that compose the film and $[\epsilon]$ is the stopping power of the alpha particles when they interact with the atoms of each element in the sample.

Table 1 shows the thickness of the ZnO films deposited by spray pyrolysis and doped with Mn, for the substrate temperatures (400, 450 and 500 °C). The results indicate that the materials synthesized at 400 and 450 °C have almost the same thickness; nevertheless at 500 °C the thickness of the sample is increased.

Figure 1 shows a RBS spectrum of a Mn-doped ZnO sample. The spectrum shows a thin film composed by Zn, O and Mn and a substrate composed with Si and O.

The spectra of the different samples presented in this study look similar to the one displayed in Fig. 1. The main differences observed come from variations in heights of Zn and the O peaks, which are directly related with their concentrations in the films. The concentration of the elements that compose the film were obtained using the SIMNRA code [13].

RBS results also show that stoichiometry of the films are related to the temperature of the substrate, resulting the most stoichiometric film the one deposited at 450 °C. Figure 2 shows that the atomic concentration of Zn presents a minimum value for the sample deposited at 500 °C; nevertheless

Table 1 RBS ZnO thin films' thickness measurements for different substrate temperatures

Substrate temperature (°C)	Thickness (nm)
400	74 ± 4
450	69 ± 3
500	105 ± 5

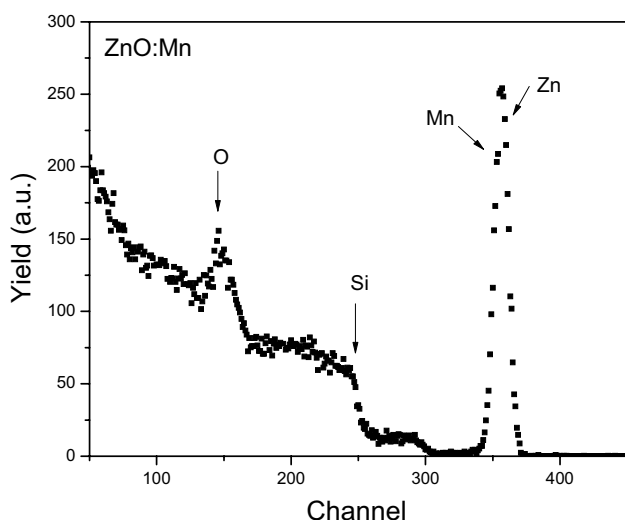


Fig. 1 RBS spectrum of a Mn-doped ZnO film

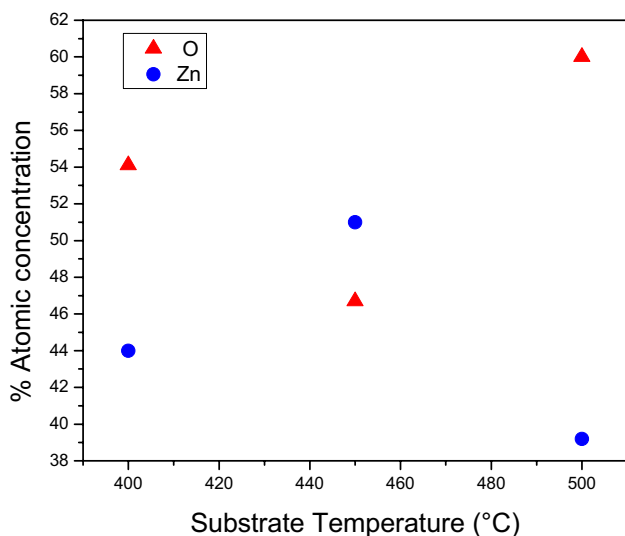


Fig. 2 Zinc and oxygen atomic concentrations versus Substrate Temperature for Mn-doped ZnO films

the behavior is opposite in the case of O concentration. This behavior can be related to the results of Table 1, where the thickness of the films are depicted. It seems that the thickness values are related to the stoichiometry of the materials, producing a decrease in thickness as the film becomes more stoichiometric. In this way the different layers that compose the more stoichiometric samples tend to grow in a more stable and order way, creating thinner films.

RBS spectra analysis also showed the presence of Zn traces into the soda lime substrate, indicating the diffusing of Zn atoms into the matrix. The major and deeper traces of Zn in matrix were observed when the film was deposited at

the higher temperature (500 °C). This is an expected result since a higher temperature in the system tends to move the atoms inside the material, easing their diffusion through the matrix.

3.2 Structural properties of Mn-doped ZnO thin films

The crystalline structure of the deposited ZnO thin films doped with Mn and synthesized at 400, 450 and 500 °C, were conducted by XRD analysis. The results, which are depicted in Fig. 3, show the undoped and Mn-doped ZnO films. The diffractograms show that the undoped and Mn-doped films are polycrystalline with a hexagonal wurtzite structure [15] and their growth orientation is along c-axis in all cases. The peaks positions are indexed to (100), (002), (101), (102), (110) and (103) [16]. An important observation is that after Mn-doping, any extra diffraction peak coming from Mn phases was observed, which means that during substitution of Zn by Mn ions in ZnO, the wurtzite structure maintained unchanged.

XRD results also show that our material grows along the (002) orientation, which is the peak with major intensity in the diffractograms. This behavior is due to the low surface-free energy of (002) plane. The increment of (002) peak with temperature can be explained as the atoms tend to migrate to positions with lowest energy, produced by the higher kinetic energy, increasing film growth at c-axis orientation. This result was remarked by Mahmood et al. [17] and Marotti et al. [18]. It has also been reported that ZnO films prepared with isopropanol or ethanol solvents exhibit high intensity of the (002) diffraction peak, making this material important for applications in optoelectronics [19].

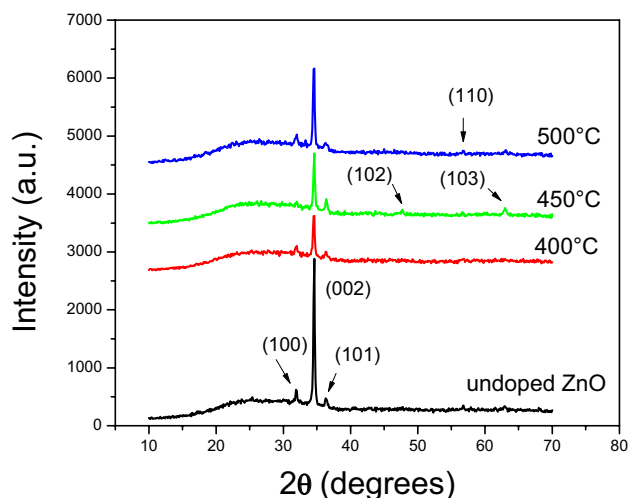


Fig. 3 XRD patterns of the undoped and Mn-doped ZnO thin films deposited at 400, 450 and 500 °C

When comparing these XRD patterns with the ones of the undoped ZnO films published in a previous work [20], the following results can be summarized. An observation of (002) peak reveals that when the substrate temperature increases, the diffraction intensity of (002) peaks of the Mn-doped ZnO films becomes weaker, relative to those of the pure ZnO. This fact indicates that as temperature is increased, the orientation of the undoped ZnO sample along (002) direction was disturbed when Mn was incorporated. This behavior is especially observed at 500 °C. It might be possible that at this temperature the Mn atoms act as obstacles (traps or dispersion centers) when ZnO is growing along (002) direction, resulting in a deterioration of the film crystallinity. This fact has been reported in many works [21, 22], independently of the film's preparation method. The comparison of the XRD patterns also shows that the peaks of the Mn-doped films are a little bit shifted to lower angle compared with the undoped ZnO films. According to Baghdad et al. [6], this shift could be a consequence of micro-strain in the structure, due to vacancies, stacking faults and interstitials.

The observed lattice constants for hexagonal ZnO:Mn were calculated from XRD patterns of Fig. 3 and by Eq. (2). The results are shown in Table 2. In this table, a comparison of the ZnO:Mn and undoped ZnO lattice constants presented in a previous work [20] is shown.

$$\frac{1}{d_{(hkl)}^2} = \frac{3}{4} \left(\frac{h^2 + hk + k^2}{a^2} \right) + \frac{l^2}{c^2} \quad (2)$$

The data of Table 2 show that lattice constants for the Mn-doped ZnO films presents a slightly increase compared to the undoped ZnO particles for all the substrate temperatures. During the incorporation of Mn²⁺ ions to ZnO films, the lattice constants for the Mn-doped films enhance as Mn²⁺ radius (0.74 Å) is a little bit larger than the Zn²⁺ (0.67 Å) and tends to expand the lattice parameter. This behavior has been reported by other groups independently of the method used to prepare the Mn-doped ZnO thin films [5, 22, 23].

As well as the lattice constants, XRD patterns give information of the average crystallite size (D). This quantity was obtained with the Scherrer's formula [24] for the ZnO films doped with Mn:

$$D = \frac{k\lambda}{\beta \cos \theta} \quad (3)$$

where k is the shape factor (0.9), λ is the wavelength of the Cu K α , β is the full width at half maximum (FWHM) of the most intense peak of the XRD spectrum and θ is the Bragg angle.

The data show that the average crystallite size of the Mn-doped ZnO increase with substrate temperature, as has been observed by Ahmed in his work [23], indicating that temperature eases the nucleation of the crystallites during the synthesis process. The crystallite size values are 30.02, 32.76 and 35.91 nm for the substrate temperature of 400, 450 and 500 °C, respectively.

3.3 SEM results

Figure 4 shows SEM micrographs of the surface morphology and grain size of the Mn-doped ZnO films at substrate temperature of (a) 400 °C, (b) 450 °C and (c) 500 °C. From the micrographs a total coverage of the substrate with ZnO grains can be appreciated. The SEM images reveal that the particles of all the samples are of nanometer size and that their density, size and shape are clearly dependent on substrate temperature. Particles change from a small spherical-like form at 400 °C to a flake-like form at 500 °C. It can be noticed in Fig. 4a that the film is a combination of rounded-like particles and amorphous material, which indicates that 400 °C is the minimum temperature necessary to form the ZnO film. At lower temperature, the material is practically amorphous. XRD results showed in Fig. 3 agree with the shape of the particles presented in Fig. 4, since narrower peaks correspond to samples with rounded shape particles. In our case, the sample deposited at 400 °C presents the narrower diffraction (002) peak and shows rounded-like particles. As deposition temperature increases to 450 °C, the FWHM of the (002) peak increases and the particles starts to lose its roundness. At 500 °C, the FWHM of (002) increases again and the shape of the particles changes completely, until becoming a flake-like shape.

J-Image code was used to measure the size of the particles of the films. A tendency of increasing the particle size with substrate temperature is observed. The average particle size is 71.28 nm for the films synthesized at 400 °C; meanwhile the samples deposited at 450 °C and 500 °C show average particle

Table 2 Comparison of lattice constants of Mn-doped ZnO (ZnO:Mn) and undoped ZnO (ZnO) films [20], prepared at temperature ranging from 400 to 500 °C

Substrate temperature (°C)	a (nm) ZnO	c (nm) ZnO	a (nm) ZnO:Mn	c (nm) ZnO:Mn
400	0.3357	0.5444	0.3362	0.5449
450	0.3365	0.5431	0.3368	0.5443
500	0.3372	0.5439	0.3375	0.5448

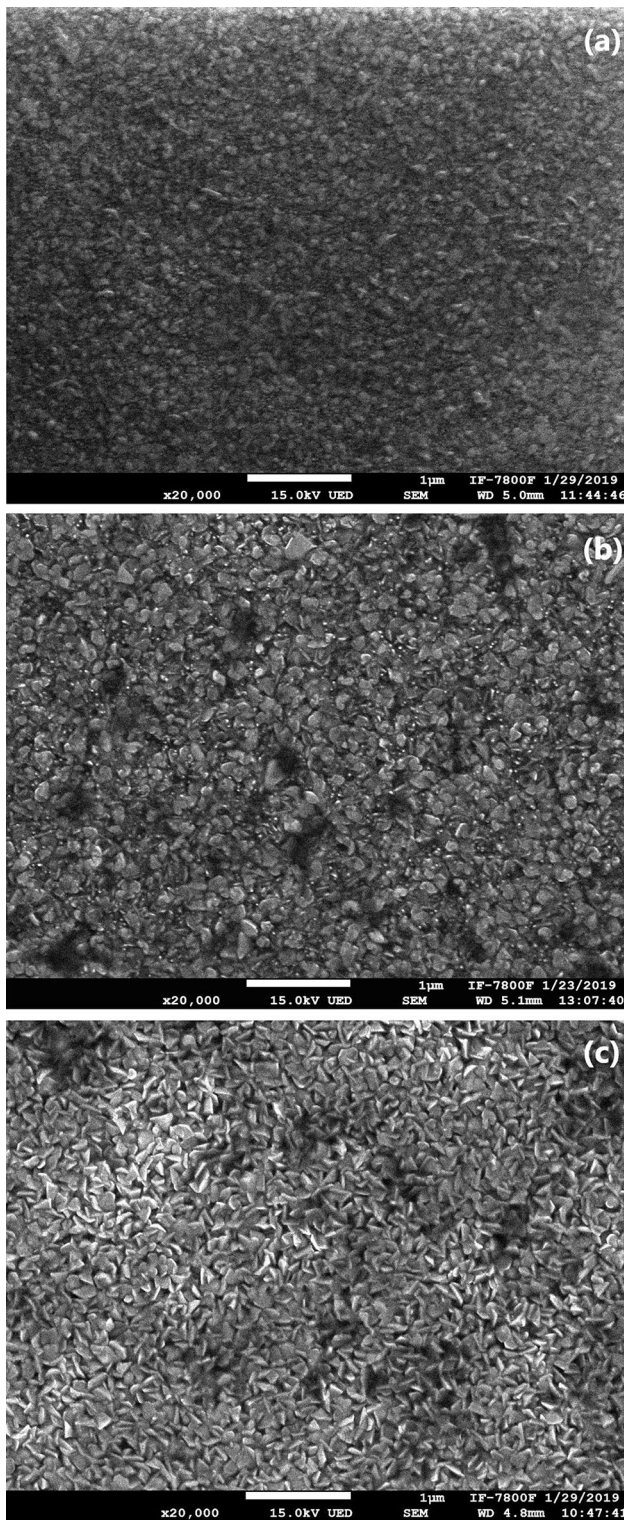


Fig. 4 SEM micrographs of ZnO:Mn films prepared at (a) 400, (b) 450 and (c) 500 °C

size of 128.75 nm and 180.01 nm, respectively. Based on these results, we can assume that substrate temperature could be used for tailoring the size of the particles that form the Mn-doped ZnO thin films.

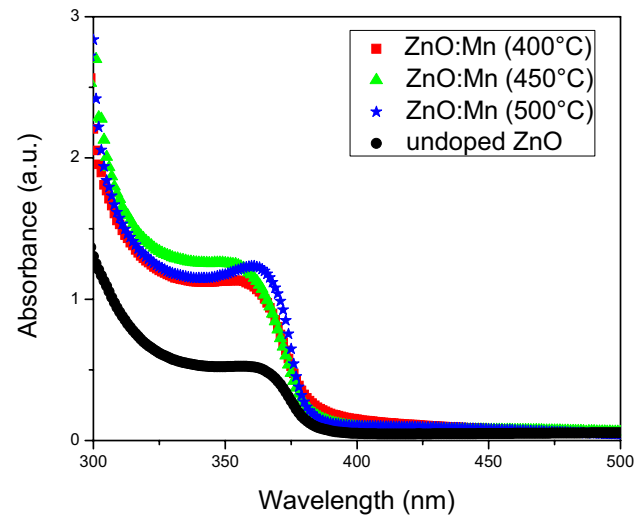


Fig. 5 Variation of absorption with wavelength of undoped and Mn-doped ZnO films

When comparing these micrographs with the ones of the undoped ZnO thin films, reported in a previous work [20], we observed that the incorporation of Mn to the films allows the nucleation and the formation of the grains that compose the ZnO films.

3.4 Optical properties

Optical absorption spectra of undoped and Mn-doped ZnO films measured at room temperature is observed in Fig. 5. The results show that the undoped ZnO thin film presents lower absorption in the visible range of the spectrum and that absorbance increases after Mn doping. This behavior has been observed by Shinde et al. [25] and may be a consequence of the introduction of Mn defects states within the forbidden band, leading to the absorption of incident photons.

It is also observed that the position of the absorption spectra in the Mn-doped ZnO film deposited at 500 °C is slightly shifted to longer wavelength. Kim et al. [26] have worked with ZnO films doped with Co and have reported a similar behavior. They assume that this shift is due to the absorption of higher-energy photons that produce activation of “spd” exchange interactions and “dd” transitions. They also reported in their work that this response of the material, led the enhancement of ferromagnetic properties.

Transmittance spectra of Mn-doped ZnO thin films deposited at different substrate temperature in the spectral range of 300–1100 nm is displayed in Fig. 6. The films are highly transparent, above 80%, in visible region. The maximum transparency is observed for the sample deposited at 500 °C, where almost a 100% of transmittance is detected. Figure 6 also shows an absorption edge around 360 nm due

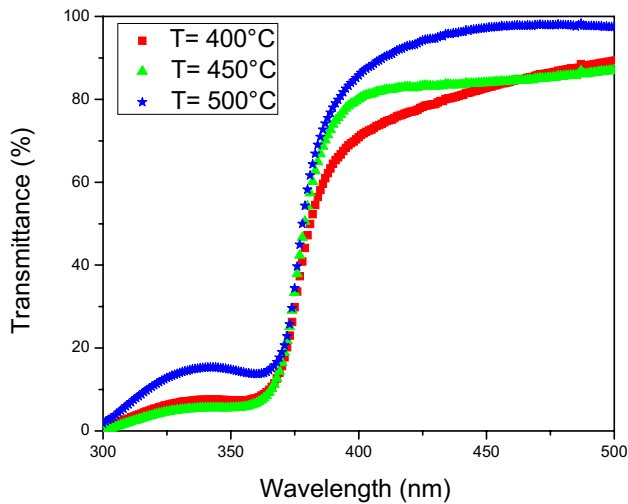


Fig. 6 Optical transmittance spectra of the Mn-doped ZnO films

to band gap absorption. This increment of transmittance with temperature is due to a decrease in optical scattering [17], which is related with an increase in the grain size of the materials and the reduction in density of grain boundaries in the films. This fact can be confirmed with the results previously presented in Sect. 3.3, where average particle size was obtained. The results show that an increase in grain size is related to a temperature increment.

The optical band gap value was calculated with the absorption coefficient (α), obtained from the transmission spectra. The variation of the absorption coefficient with photon energy ($h\nu$) obeys Tauc relation. Equation 4 [27] calculates the optical band gap for an allowed direct transition:

$$(\alpha h\nu) = A(h\nu - E_g)^{1/2} \quad (4)$$

where E_g is the optical band gap and A is a constant related to the refractive index of the material.

To obtain the optical band gap values of the materials, the linear part of the plots of $(\alpha h\nu)^2$ versus $h\nu$ to $\alpha = 0$ must be extrapolated. The extrapolation for the three substrate temperatures is shown in Fig. 7.

The evaluated band gap energies of Mn-doped ZnO films synthesized at 400, 450 and 500 °C are depicted in Fig. 8. The results indicate that the band gap energy is dependent upon the growth temperature and shows a blue shift as substrate temperature increases, approaching a value of 3.27 eV for 500 °C. Blue and red shifts of the energy gap as a function of the growth temperature have been reported by other groups. For instance Bentes, et al. [28] and Zhao et al. [29] reported a red shift of the energy band gap as temperature increases; meanwhile Shan et al. [30] and Khaliq, et al. [17] observed the opposite, which is consistent with the results that were found in this work. The possible mechanisms that

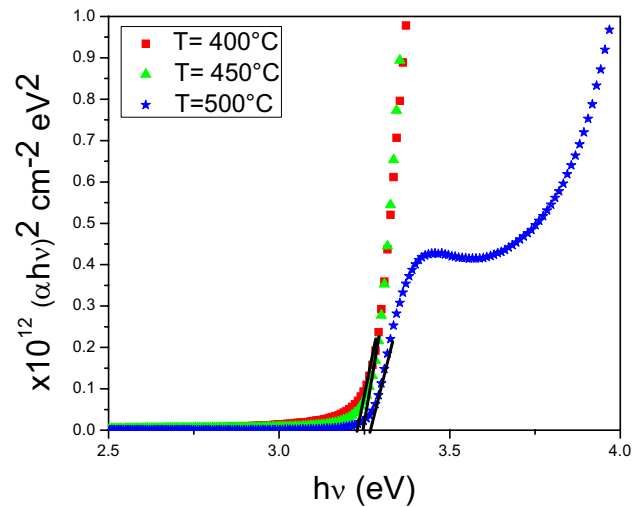


Fig. 7 Energy band gap of ZnO:Mn thin films prepared at different substrate temperatures

can cause the changes in energy band gap are variation in crystallinity, changes in density of impurities, defects, quantum size effects and crystallite dimensions.

In our case crystallite dimensions might be the mechanism behind the measured changes in optical band gap as crystallite size varies with temperature as is shown in Table 2. This result is corroborated by the group of Benramache [31] and Marotti, et al. [18]. In both cases, they observed variations in crystallite size and optical band gap as a function of substrate temperature. Hafdallah, et al. [32] attribute the blue shift in optical band gap, when substrate temperature is increased, to an improvement in the film crystallinity.

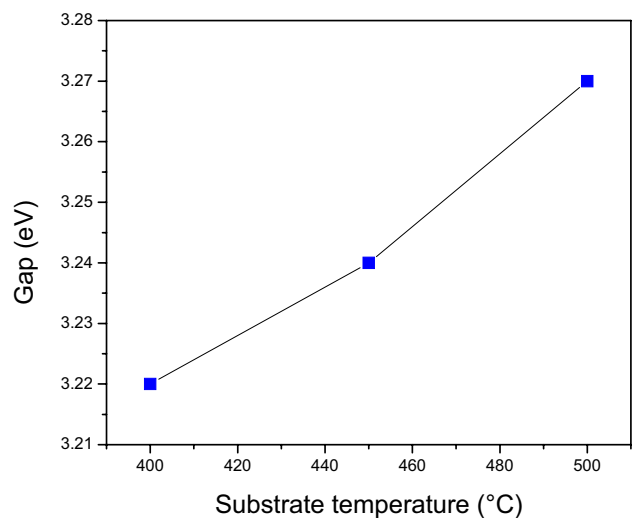


Fig. 8 Optical band gap of Mn-doped ZnO thin films prepared at different substrate temperatures

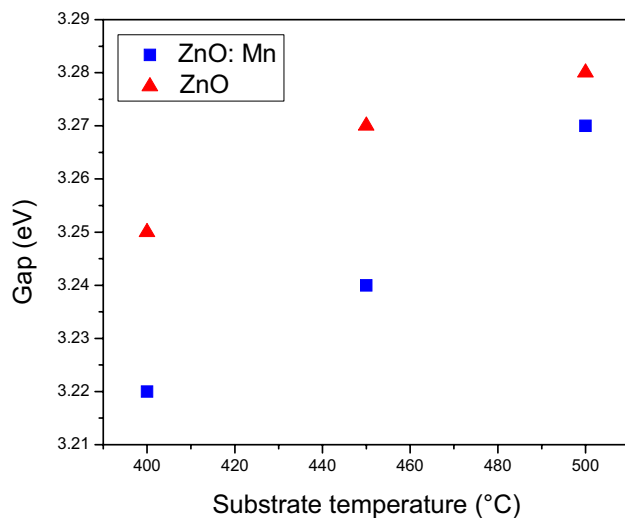


Fig. 9 Optical band gap of undoped (ZnO) [20] and Mn-doped ZnO (ZnO:Mn) thin films prepared at different substrate temperatures

The incorporation of Mn to the ZnO films produces a decrease in the band gap energy for all the substrates temperatures, as is observed in Fig. 9. The red shift in the energy band gap of ZnO when Mn is incorporated to the film is due to the *s-d* and *p-d* exchange interactions. The *s-d* interactions give place to a negative correction to the conduction band energy; meanwhile the *p-d* interactions give rise to a positive correction to the valence band energy, leading to a narrower band gap [33]. This narrowing in the band gap is attributed to many body effects on the conduction and valence bands and can be originated from electron interaction and impurity scattering. Similar results has been reported by several research groups, such as Modal et al. [34] and Shinde et al. [25].

When comparing with other studies, we found that the optical band gap values do depend on the preparation method of the ZnO doped with Mn. The values go from 2.78 eV [35] to 3.252 eV [22] for ZnO:Mn films deposited with the solvothermal synthesis and the sol–gel method, respectively. In our case, the optical band gap value is closer to the values obtained when the films are synthesized by sol–gel method.

3.5 Electrical results

The resistivity values of the Mn-doped ZnO films are presented in Fig. 10. The resistivity shows a maximum value of $40.05 \times 10^{-2} \Omega\text{cm}$ for the 400 °C film, then the resistivity decreases and reaches a minimum value of $4.86 \times 10^{-2} \Omega\text{cm}$ for the sample synthesized at 450 °C, and finally the resistivity increases up to $23.3 \times 10^{-2} \Omega\text{cm}$ for the sample growth at 500 °C. The behavior of increasing and decreasing electrical resistivity of ZnO with deposition temperature has

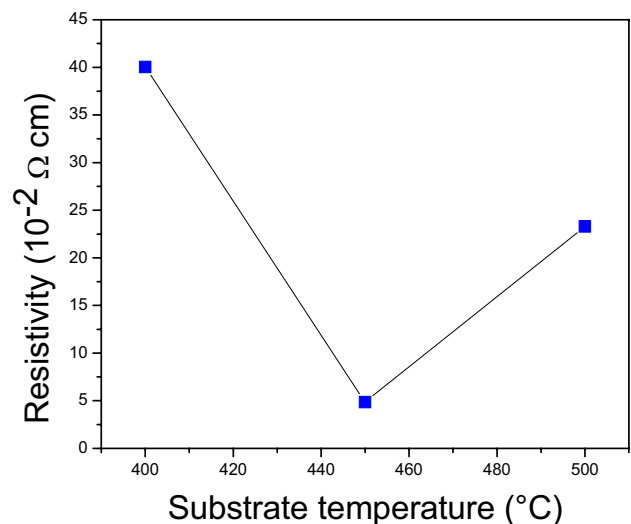


Fig. 10 Resistivity values of the Mn-doped ZnO thin films as a function of the substrate temperature

been reported by several authors. In those cases, the lowest value of resistivity is presented at different temperature, such as 300 °C [36, 37], 340 °C [38], 415 °C [39], 425 °C [40] or 450 °C [41], depending on the dopant element. In their works the authors explain this behavior using several theories. For instance Castañeda et al. [39] assumed that this behavior is a consequence of an increase of carrier concentration due to the formation of point defects; Tapatee Kundu, et al. [36] showed that the decrease in resistivity is controlled by intrinsic defects produced at high temperature; Benramache et al. [38] explained that this behavior in resistivity is due to the increase of the potential barriers because the doped atoms are segregated into the grain boundaries; meanwhile Navid Najfi et al. [41] and Muruganantham et al. [42] proposed that the increase and decrease in resistivity has its origin during film deposition, as the number of Zn and O atoms can change, getting a maximum or minimum amount of them. In this way, oxygen vacancies are created in the lattice when the amount of Zn atoms increases in the film, giving free electrons to the film. These electrons increase the charge carrier concentration, and as a consequence, the electrical resistivity decreases. This effect might be happening in our case, and can be corroborated in Fig. 2, where O concentration diminishes at 450 °C and increases at 400 and 500 °C, following the same behavior as resistivity.

A comparison of the variation of electrical resistivity with substrate temperature of Mn-doped ZnO and pure ZnO films is depicted in Fig. 11. The resistivity values show that the Mn-doped and undoped films follow the same behavior in variation of resistivity; indicating that this tendency does not depend upon Mn-doping, but it is inherent to ZnO preparation when ethanol is used. This can be confirmed since in a previous work [43] ZnO thin films were prepared using methanol instead of

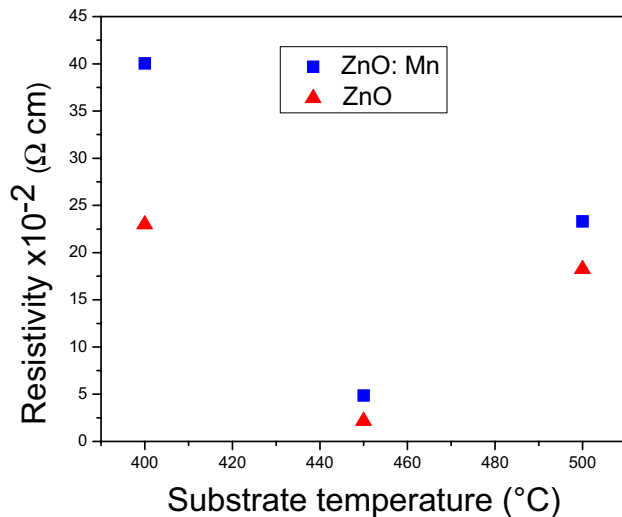


Fig. 11 Resistivity of the undoped (ZnO) [20] and Mn-doped ZnO (ZnO:Mn) films as a function of the substrate temperature

ethanol and the electrical results look completely different. Figure 11 also shows that for all the substrate temperatures, the resistivity values on the Mn-doped ZnO films are greater than the ones of the undoped films, especially for the sample deposited at 400 °C.

Electrical properties of thin films depend on several parameters, such as defects, impurities, grain size, grain boundaries and growing conditions. The increase in resistivity of Mn-doped ZnO films has been observed by several groups independently of the techniques used during preparation of ZnO thin films. For instance, Shinde et al. [25], showed that the increase in resistivity may be due to nanocrystalline nature of the films. Han et al. [44] and Rusu et al. [5] also documented this increment, arguing that a small quantity of Mn below the solubility limit in ZnO increases resistivity as it reduces the carrier concentration. In the case of electrical properties, oxygen vacancies play an important role, as their increment influences the resistivity of ZnO thin films. When ZnO thin films are doped with Mn atoms, these atoms have a tendency of accumulating in the grain boundaries, contributing the oxidation process. This fact tends to decrease the oxygen deficiencies, increasing the resistivity of the films as has been observed by Motevalzadeh et al. [21].

4 Conclusions

Mn-doped ZnO films were prepared using the spray pyrolysis technique at 400, 450 and 500 °C. Optical, electrical and structural studies were performed to the ZnO films. The results reveal an increment in transmittance with temperature, which can be due to a decrease in optical scattering, related with an increment in the grain size of ZnO and

the reduction in density of grain boundaries in the films. The energy band gap of the films shows a dependence with substrate temperature, with a blue shift for higher temperatures, and a value of 3.27 eV for 500 °C. In the case of the resistivity, it shows a maximum value at 400 °C, then it reduces considerably at 450 °C and increases again at 500 °C. The ZnO films show small variations in the lattice parameters when they are doped with Mn. This variations are due to the incorporation of Mn ions into the ZnO lattice and the substitution of Zn by Mn ions. When comparing the results of Mn-doped ZnO with undoped ZnO, the band gap decreases when Mn is incorporated to the films, due to the s-d and p-d exchange interactions. Increments in the resistivity values are present when ZnO is doped with Mn. Due to this resistivity behavior, the material seems to be an ideal candidate for applications as gas sensors.

Acknowledgements The authors want to thank the technical assistance of Roberto Hernández, Diego Quiterio, Francisco Javier Jaimes, Mauricio Escobar and Antonio Morales. This work was supported by UNAM DGAPA-PAPIIT under Grants IN 101-219 and IN 102-419.

References

1. V. Srikant, D.R. Clarke, On the optical band gap of zinc oxide. *J. Appl. Phys.* **83**, 47 (1998). <https://doi.org/10.1063/1.367375>
2. A. Tsukazaki, S. Fuke, Y. Sewaga, H. Ohno, H. Koinuma, M. Kawasaki, Repeated temperature modulation epitaxy for p-type doping and light-emitting diode based on ZnO. *Nat. Mater.* **4**, 42 (2005). <https://doi.org/10.1038/nmat1284>
3. D.M. Bagnall, Y.F. Chen, Z. Zhu, T. Yao, Optically pumped lasing of ZnO at room temperature. *Appl. Phys. Lett.* **70**, 2230 (1997). <https://doi.org/10.1063/1.118824>
4. S. Benramache, A. Arif, O. Belahssen, A. Guettaf, Study on the correlation between crystallite size and optical gap energy of doped ZnO thin film. *J. Nanostr. Chem.* **3**, 80 (2013). <https://doi.org/10.1186/2193-8865-3-80>
5. G.G. Rusu, P. Gorley, C. Baban, A.P. Rambu, M. Rusu, Preparation and characterization of Mn-doped ZnO thin films. *J. Optoelectron. Adv. Mater.* **12**, 895 (2010). <https://doi.org/10.1134/S1063783418050050>
6. R. Baghdad, B. Kharroubi, A. Abdiche, M. Vousmaha, M.A. Bezzerrouk, A. Zeinert, M. El Marssi, K. Zellama, Mn doped ZnO nanostructured thin films prepared by ultrasonic spray pyrolysis method. *Superlatt. Microstr.* **52**, 711 (2012). <https://doi.org/10.1016/j.spmi.2012.06.023>
7. Y. Aoun, B. Benhaoua, S. Benramache, A study the aluminum doped zinc oxide thin films. *J. Nano Electron. Phys.* **7**, 3006 (2015). <https://doi.org/10.1016/j.msec.2007.10.006>
8. R. Wen, L. Wang, X. Wang, G.-H. Yue, Y. Chen, D.-L. Peng, Influence of substrate temperature on mechanical, optical and electrical properties of ZnO: Al films. *J. Alloys Compd.* **508**, 370 (2010)
9. A.U. Ubale, V.P. Deshpande, Effect of manganese inclusion on structural, optical and electrical properties of ZnO thin films. *J. Alloys Compd.* **500**, 138 (2010). <https://doi.org/10.1016/j.jallcom.2010.04.004>
10. W.A. Bryant, The fundamental of chemical vapor deposition. *J. Mater. Sci.* **12**, 1285 (1977). <https://doi.org/10.1016/j.jallcom.2010.08.034>

11. M. Krunk, E. Mellikov, Zinc oxide thin films by the spray pyrolysis method. *Thin Solid Films* **270**, 33 (1995). <https://doi.org/10.1238/Physica.Topical.079a00209>
12. D. Perednis, L.J. Gauckler, Thin film deposition using spray pyrolysis. *J. Electroceram.* **14**, 103 (2005). <https://doi.org/10.1007/s10832-005-0870-x>
13. M. Mayer, SIMNRA User's Guide, Version 6.04, Max Planck-Institute für Plasmaphysik, Garching.
14. W.K. Chu, J.W. Mayer, M.A. Nicolet, *Backscattering spectrometry* (Academic Press, New York, 1978)
15. A. Zaier, F. Oum Al Az, F. Lakfif, A. Kabir, S. Boudjadar, M.S. Aida, Effects of the substrate temperature and solution molarity on the structural opto-electric properties of ZnO thin films deposited by spray pyrolysis. *Mater. Sci. Semicond. Process.* **12**, 207 (2009). <https://doi.org/10.1016/j.mssp.2009.12.002>
16. Powder Diffraction File 36–1451 for hexagonal ZnO, JCPDS-International center for Diffraction data (1997).
17. K. Mahmood, S. Bashir, M. Kaleeq-Ur-Rahman, N. Farid, M. Akram, A. Hayat, A. Faizan-Ul-Haq, Effects of substrate temperature on structural, optical and surface morphology properties of pulsed laser deposited ZnO thin films. *Surf. Rev. Lett.* **20**, 1350032 (2013). <https://doi.org/10.1142/S0218625X13500327>
18. R.E. Marotti, P. Giorgi, G. Machado, E.A. Dalchiale, Crystallite size dependence of band gap energy for electrodeposited ZnO grown at different temperatures. *Sol. Energy Mater. Sol. Cells* **90**, 2356 (2006). <https://doi.org/10.1016/j.solmat.2006.03.008>
19. G.A. Velázquez-Nevárez, J.R. Vargas-García, J. Aguilar-Hernández, O.E. Vega-Becerra, F. Chen, Q. Shen, L. Zhang, Optical and electrical properties of (002)-oriented ZnO films prepared on amorphous substrates by sol-gel spin-coating. *Mater. Res.* **19**, 113 (2016). <https://doi.org/10.1590/1980-5373-mr-2016-0808>
20. D. Acosta, A. López-Suárez, C. Magaña, F. Hernández, Structural, electrical and optical properties of ZnO thin films produced by chemical spray using ethanol in different amounts of the sprayed solution. *Thin Solid Films* **653**, 309 (2018). <https://doi.org/10.1016/j.tsf.2018.03.031>
21. L. Motevalizadeh, B.G. Shohany, M.E. Abrishami, Effects of Mn doping on electrical properties of ZnO thin films. *Mod. Phys. Lett. B* **4**, 1650024 (2016). <https://doi.org/10.1142/S021798491650024X>
22. S. Yang, Y. Zhang, Structural, optical and magnetic properties of Mn-doped ZnO thin films prepared by sol-gel method. *J. Magn. Magn. Mater.* **334**, 52 (2013). <https://doi.org/10.1016/j.jmmm.2013.01.026>
23. S.A. Ahmed, Structural, optical and magnetic properties of Mn-doped ZnO samples. *Results Phys.* **7**, 604 (2017). <https://doi.org/10.1016/j.rinp.2017.01.018>
24. A. Rahal, S. Benramache, B. Benhaoua, Substrate temperature effect on optical property of ZnO thin films. *Eng. J.* **18**, 81 (2014). <https://doi.org/10.4186/ej.2014.18.2.81>
25. V.R. Shinde, T.P. Gujar, C.D. Lokhande, R.S. Mane, Sung-Hwan Han, Mn doped and undoped ZnO films: a comparative structural, optical and electrical properties study. *Mater. Chem. Phys.* **96**, 326 (2006). <https://doi.org/10.1016/j.matchemphys.2005.07.045>
26. K.J. Kim, Y.R. Park, Spectroscopic ellipsometry study of optical transitions in Zn_{1-x}Co_xO/Zn_{1-x}Co_xO alloys. *Appl. Phys. Lett.* **81**, 1420 (2002). <https://doi.org/10.1063/1.1501765>
27. B.D. Vezbicke, S. Patel, B.E. Davis, D.P. Birnie III, Evaluation of the Tauc method for optical absorption edge determination: ZnO thin films as a model system. *Phys. Status Solid B* **252**, 1700 (2015). <https://doi.org/10.1002/pssb.201552007>
28. L. Bentes, R. Ayouchi, C. Santos, R. Schwarz, P. Sanguino, O. Conde, M. Peres, T. Monteiro, O. Teodoro, ZnO films grown by laser ablation with and without oxygen CVD. *Superlatt. Microstr.* **42**, 152 (2007). <https://doi.org/10.1016/j.spmi.2007.04.049>
29. J.L. Zhao, X.M. Li, J.M. Bian, W.D. Yu, X.D. Gao, Structural, optical and electrical properties of ZnO films grown by pulsed laser deposition (PLD). *J. Cryst. Growth* **276**, 507 (2005). <https://doi.org/10.1016/j.jcrysgro.2004.11.407>
30. F.K. Shan, G.X. Liu, W.J. Lee, I.S. Kim, B.C. Shin, Y.C. Kim, Transparent conductive ZnO thin films on glass substrates deposited by pulsed laser deposition. *J. Cryst. Growth* **277**, 284 (2005). <https://doi.org/10.1016/j.jcrysgro.2005.01.016>
31. S. Benramache, O. Belahssen, A. Arif, A. Guettaf, A correlation for crystallite size of undoped ZnO thin film with the band gap energy-precursor molarity-substrate temperature. *Optik* **125**, 1303 (2014). <https://doi.org/10.1016/j.ijleo.2013.08.015>
32. A. Hafdallah, A. Ferdi, M.S. Aida, N. Attaf, A. Amara, Effect of substrate temperature studies on spray pyrolysis deposited ZnO thin films. *Int. J. Adv. Res.* **3**, 240 (2015). <https://doi.org/10.1515/msp-2015-0062>
33. Y.R. Lee, A.K. Ramdas, R.L. Aggarwal, Energy gap, excitonic, and "internal" Mn²⁺ optical transition in Mn-based II-VI diluted magnetic semiconductors. *Phys. Rev. B* **38**, 10600 (1988). <https://doi.org/10.1103/PhysRevB.38.10600>
34. S. Modal, S.R. Bhattacharyya, P. Mitra, Preparation of manganese-doped ZnO thin films and their characterization. *Bull. Mater. Sci.* **36**, 223 (2013). <https://doi.org/10.1007/s12034-013-0462-3>
35. S. Senthilkumaar, K. Rajendran, S. Banerjee, T.K. Chini, V. Sengodan, Influence of Mn doping on the microstructure and optical property of ZnO. *Mater. Sci. Semicond. Process.* **11**, 6 (2008). <https://doi.org/10.1016/j.mssp.2008.04.005>
36. T.K. Roy, D. Sanyal, D. Bhowmick, A. Chakrabarti, Temperature dependent resistivity study on zinc oxide and the role of defects. *Mater. Sci. Semicond. Process.* **16**, 332 (2013). <https://doi.org/10.1016/j.mssp.2012.09.018>
37. Y.-L. Lee, S.-F. Chen, C.-L. Ho, M.-C. Wu, Effects of oxygen plasma post-treatment on Ga-doped ZnO films grown by thermal-mode ALD. *ECS. J. Solid State Sci. Technol.* **2**, 316 (2013). <https://doi.org/10.1149/2.024307jss>
38. S. Benramache, B. Benhaoua, F. Chabane, Effect of substrate temperature on the stability of transparent conducting cobalt doped ZnO thin films. *J. Semicond.* (2012). <https://doi.org/10.1088/1674-4926/33/9/093001>
39. L. Castañeda, A. Maldonado, A. Escobedo-Morales, M. Avenadoño-Alejo, H. Gómez, J. Vega-Pérez, M. de la L. Olvera, Indium doped zinc oxide thin films deposited by ultrasonic spray pyrolysis technique: Effect of the substrate temperature on the physical properties. *Mater. Sci. Semicond. Process.* **14**, 114 (2011). <https://doi.org/10.1016/j.mssp.2011.01.013>
40. A. Ashour, M.A. Kaid, N.Z. El-Sayed, A.A. Ibrahim, Physical properties of ZnO thin films deposited by spray pyrolysis technique. *Appl. Surf. Sci.* **252**, 7844 (2006). <https://doi.org/10.1016/j.apsusc.2005.09.048>
41. N. Najfi, Seyed Mohammad Rozait, Resistivity reduction of nanostructured undoped zinc oxide thin films for Ag/ZnO bilayers using APCVD and sputtering techniques. *Mater. Res.* **21**, e20170933 (2018). <https://doi.org/10.1590/1980-5373-mr-2017-0933>
42. G. Muruganantham, K. Ravichandran, K. Saravanakumar, K. Swaminathan, N. Jabena Begum, B. Sakthivel, Effect of solvent volume on the physical properties of sprayed fluorine-doped zinc oxide thin films. *Cryst. Res. Technol.* **47**, 429 (2012). <https://doi.org/10.1002/crat.201100527>
43. A. López-Suárez, D. Acosta, C. Magaña, F. Hernández, Effect of substrate temperature and sprayed methanol on nanostructure, optical and electrical properties of ZnO films. *Adv. Sci. Eng. Med.* **10**, 105 (2018). <https://doi.org/10.1166/ase.2018.2181>
44. J. Han, P.Q. Mantas, A.M.R. Senos, Defect chemistry and electrical characteristics of undoped and Mn-doped ZnO. *J. Eur. Ceram. Soc.* **22**, 49 (2002). <https://doi.org/10.1016/S0955-2219>